Geophys.J. Int. (2007) **XXX,** 000-000

An improved UK local magnitude scale from analysis of shear- and Lg-wave amplitudes

David C. Booth

British Geological Survey, Murchison House, West Mains Road, Edinburgh EH9 3LA, UK.
E-mail: dcb@bgs.ac.uk

Abbreviated title: UK shear- & *Lg*-wave amplitudes

Author's contact details:

Dr David C. Booth

British Geological Survey

Murchison House

West Mains Road

Edinburgh EH9 3LA

UK.

Tel: 0131 650 0219

Fax: 0131 667 1877

E-mail: dcb@bgs.ac.uk

An improved UK local magnitude scale from analysis of shear- and Lg-wave amplitudes

David C. Booth

British Geological Survey, Murchison House, West Mains Road, Edinburgh EH9 3LA, UK. E-mail: dcb@bgs.ac.uk

SUMMARY

The amplitudes of shear-waves and *Lg*-waves recorded at UK seismograph stations from local earthquakes in the range 0-600km have been subjected to an analysis of variance, allowing separation of the effects of earthquake size, distance and station corrections for each recording site. The propagation paths sample mainly the central to western part of the UK, with good north to south coverage. The analysis of 385 amplitude readings at 28 stations from 40 earthquakes showed that the effects of both distance and station (site) corrections were statistically significant. Tables of corrections for both distance and station effects have been derived to allow local magnitude *ML* to be determined more accurately from horizontal and vertical component records. One set of tables allows the estimation of an *ML* which is consistent with the original Richter definition of *ML*, with a standard deviation which is smaller than that produced by the theoretical attenuation curve, defined according to attenuation in Southern California, which has customarily been used to calculate *ML* in the UK. The reduction in standard deviation is mainly due to the incorporation of station terms to correct for station effects, since the theoretical and observed variations of attenuation with distance are similar. This similarity implies that Southern California and the UK show a similar variation of distance-dependent attenuation for *Lg* waves, which was not expected in view of the differences in geology and tectonics. Another set of tables is provided to calculate an *ML* which is consistent with the body wave magnitude m_b determined by the International Data Centre (IDC) from station records of the Comprehensive Test-Ban Treaty Organisation's global monitoring network. The decay with distance of the predominantly *Lg*-wave amplitude values gives a value of 440 ± 50 for *Lg* Q at a frequency of 3 Hz, in agreement with estimates obtained from spectral displacement amplitudes of *Lg*-waves in the UK.

Key Words: S-waves, surface waves, attenuation, statistical methods

1 INTRODUCTION

Magnitude is one of the most important parameters associated with a seismic event. It is an objective measure of earthquake size, using instrumental measurements of ground motion with corrections for epicentral distance. Seismic wave amplitude attenuates with increasing distance, and so an appropriate distance correction must be applied to a ground motion amplitude measurement to provide a magnitude estimate. In the distance range 0°-20°, attenuation occurs in the crust and upper mantle and is region-dependent, and therefore a distance correction which takes account of regional attenuation characteristics is required in any procedure to generate a magnitude value from wave amplitude measurements in this distance range.

The British Geological Survey (BGS) estimates the magnitude of earthquakes occurring in the region of the UK using a local magnitude *ML.* This scale is the same as that defined by Hutton & Boore (1987), following earlier work by Richter (1935), which uses the maximum trace amplitudes recorded on standard Wood-Anderson horizontal seismometers. The BGS uses Willmore Mk3 seismometers rather than Wood-Anderson seismometers, but using the responses of the two instruments, amplitudes are measured from equivalent Wood-Anderson seismograms. This is done by a process of deconvolving the Willmore response from the Fourier transform of the seismogram and convolving the result with the Wood-Anderson response, then taking the inverse Fourier transform to give the Wood-Anderson seismogram.

BGS have always calculated local magnitude following Richter (1935) by calculating the logarithm of the maximum wave amplitude recorded on each of two orthogonal horizontal seismometers, adding the same correction to each to allow for epicentral distance, and taking the mean of the two component magnitudes. The maximum trace amplitude is almost always in the shear-wave coda and corresponds to the crustal shear wave *Sg*, or the multiply reflected shear wave group *Lg* which follows the *Sg* wave onset. Some agencies form the average of the two maximum horizontal component amplitudes, and use that to calculate the magnitudes; this convention differs from that of Richter and will result in a systematic difference in magnitudes. Richter's (1935) procedure differs from the modern recommendation which is given in the New Manual of Seismic Observatory Practice (NMSOP) (Bormann 2002). NMSOP suggests that where horizontal component records are used, amplitudes should be measured at the same time, so that the amplitudes can be combined vectorially, and the largest vectorially combined value is used to form the magnitude. The latter approach should be adopted where a magnitude scale is being developed for a new station or network. However, for reasons of continuity in their earthquake bulletins, BGS continue to use Richter's procedure as described above.

Hutton and Boore (1987) have published a correction for distance which is based on observations in California, and the BGS has applied this correction when estimating local magnitude using amplitude measurements from its UK seismic monitoring network stations. The BGS recognises that seismic wave attenuation characteristics are likely to differ between California and the UK, so that application of the Hutton and Boore correction for the effect of attenuation of amplitude with distance will result in calculated local magnitudes being biased in some way with respect to those determined by independent global magnitude scales.

The UK region is seismically active, but earthquakes of magnitude greater than 4.0 are less frequent than one per year (with the exception of the North Sea Graben region), and the UK seismic monitoring network is primarily designed for the detection and analysis of relatively low magnitude seismic events. Until recently, technical limitations imposed by the low dynamic range of the UK seismic network recording system meant that shear-wave amplitudes were often not measurable at stations near the epicentre when any relatively large (ML>3.5) earthquake occurred, due to saturation of the recording system. For many years, this restriction limited the amount of data available for wave amplitude studies over a wide distance range, since small seismic events are observable only over a limited distance range. However, as instrumentation has improved, and a network of strong motion accelerometer stations has been installed, sufficient data have become available for such a study.

Often local effects associated with a particular recording site are present, and these may also bias the determination of magnitude at a station. These include seismometer-ground coupling, soil amplification, path azimuth, topographic and focussing effects, local geology and attenuation. These shall be referred to as station effects, and will be corrected for using station corrections. In this report, I apply an analysis of variance technique used by Carpenter et al.

(1967) and others to determine an amplitude-distance curve and station corrections for shear-wave amplitudes recorded at UK short-period seismic stations in the range 0-600km. I then use Hutton and Boore's criteria, adapted from Richter (1935), to calibrate the correction to give a local magnitude based on observed amplitude values at UK stations, which is consistent with Richter's original definition. The corrections are also calibrated against independent measurements of m_b derived for the UK earthquakes which are listed in the Reviewed Event Bulletins of the International Data Centre (IDC), Vienna. The result is a distance correction table which is appropriate for estimating a local magnitude *ML* equivalent to m_b(IDC). The table is derived not because the IDC magnitude is especially representative for UK earthquakes, but because there is no existing relation between UK *ML* and m_b(IDC).

The IDC is operated by the Comprehensive (nuclear) Test Ban Treaty Organisation (CTBTO) for the production and distribution of data for CTBT verification. The identification of a seismic event as an explosion from the use of seismograms alone is vital in monitoring compliance with the CTBT, since seismic techniques are required to monitor underground nuclear explosions. Explosions must be discriminated from much more commonly occurring earthquakes; this is a difficult task and no single discrimination technique has been found which is successful for all seismic events. Probably the most successful technique so far has been the m_b:M_S criterion (Marshall & Basham 1972) , which depends on the observation that for a seismic event with a given body wave magnitude m_b, the surface wave magnitude M_S is typically larger for an earthquake than for an explosion. Application of the criterion requires that accurate measurements of m_b and M_S are available. For small events, m_b<4.0, few if any measurements of m_b and M_S may be available. For such events, the ability to determine an equivalent m_b from locally recorded amplitudes may be useful, particularly for a state signatory which wishes to provide supporting discriminatory evidence in respect of a nearby event. It is therefore useful that a reliable estimate of m_b for local events can be made, using seismic wave amplitudes recorded at local stations. Estimates of m_b consistent with those obtained by the IDC are formed, and compared with those of the USGS National Earthquake Information Centre (NEIC), International Seismological Centre (ISC), and an empirical relation derived by Neilson & Burton (1985).

The decay of log A as a function of distance allows the calculation of an average Q for the UK for the measured waves of maximum amplitude. Examination of the particle motion of these waves indicates that they are predominantly *Lg* waves, arriving shortly after the *Sg* phase, a sequence of shear waves multiply reflected within the crust, which can alternatively be described as a superposition of higher mode surface waves. There is a wealth of surface wave attenuation work in the literature, such as Brune (1962), Nuttli (1973) and Burton (1974), following Ewing et al. (1957), and many *Lg* attenuation studies exist, of which Ottemöller et al. (2002), Benz et al. (1997), Bowman & Kennett (1991), Herrmann (1980) are only a few examples. *Lg* waves provide a good measure of path-averaged crustal properties, in particular S-wave velocity and attenuation. Studies of wave attenuation in the crust under the UK have mainly been confined to the shallow crust. MacBeth and Burton (1985, 1986, 1987, 1988) conducted a series of surface wave studies in the UK. While most of these were based on data from explosions, and pertain to the shallow crust, in one study (MacBeth and Burton, 1985), data from a 11 km deep earthquake observed on a lithospheric seismic profile in Britain (LISPB) allowed a shear velocity-depth profile to be determined, showing a consistent increase in velocity from 3.4 to 3.7 km s^{-1} in a depth range from 2 to 17 km. The group velocities corresponding to the maximum amplitude arrivals in the present study vary between 2.4 and 4.4 km s^{-1}, with most values in the 3.2 to 3.6 km s^{-1} range. The focal depths of the UK earthquakes used in this study vary between 0.1 and 26.4 km (the average depth was 11.7 km) and hypocentral distances range from 19 to over 800 km, thus it is probable that the full range of crustal depths is sampled by the *Lg* waves. Observations of amplitude decay with distance are used to derive a value for Q for the dominant period of *Lg* waves over the distance range 110 and 390 km in the UK.

2 METHOD OF ANALYSIS

Following Carpenter et al. (1967) and Booth et al. (1974), we write the amplitude of the shear-wave or *Lg* wave recorded at a seismometer station as

$$\log_{10}A = b + s + r \tag{1}$$

where A is the maximum wave amplitude recorded on the seismometer, b is a term proportional to source size, s is a station effect, and r is a distance effect. The formula for local magnitude ML according to Richter (1935) is

$$ML = \log_{10}A \ - \ \log_{10}A_{0,} \tag{2}$$

where $-\log_{10}A_0$ is a correction for the effect of distance, abbreviated here to the distance-dependent function $B(\Delta)$. To allow for the possible effect of local station effects we introduce a station term S. Then

$$ML = \log_{10}A + B(\Delta) + S \tag{3}$$

It follows that

$$\log_{10}A = ML - B(\Delta) - S \tag{4}$$

and $\log_{10}A$ can be expressed as a sum of effects of source size, distance, and recording site.

To analyse the data I follow Carpenter et al. (1967) and Booth et al. (1974) and make the assumption that if a_{ijk} is $\log_{10}A$ for the j-th station and the i-th earthquake in the k-th distance range then

$$a_{ijk} = b_i + s_j + r_k + c + e_{ijk} \tag{5}$$

where b_i is a measure of the size (energy release) of the i-th earthquake, s_j is the station effect for the j-th station, r_k is the effect of distance, c is a constant, and e_{ijk} is an error. b_i, s_j, r_k and c can be estimated in the presence of this error by the method of least squares (on the assumption that the errors have zero mean) with the conditions

$$\Sigma b_i = \Sigma s_j = \Sigma r_k = 0, \tag{6}$$

where b_i is summed over n earthquakes, s_j is summed over q stations, and r_k is summed over l distance ranges. Condition (6) is applicable due to the linear dependence of the terms in equation (5), and introduction of the constant c permits the application of this condition. The average values of b_i , s_j and r_k are set to zero and their true values become a matter of definition. By making the additional assumption that the errors e_{ijk} are normally distributed, confidence limits can be determined for b_i , s_j , and r_k . The problem corresponds to an analysis of variance of three effects: earthquake size, distance and station. The distance correction $B(\Delta)$ and station correction S in (3) are derived from the distance and station effects, s_j and r_k respectively. We can write

$$B(\Delta) = \ -r_k + D, \tag{7}$$

where D is a constant term which is added so that the magnitudes ML computed using the revised curve agree on average with magnitudes computed by a specified agency. This gives the term $B(\Delta)$ in (3); the station correction S which is to be added to $\log_{10}A$ and $B(\Delta)$ in (3) to form ML is $-s_j$. Also, from (3),

$$ML = \log_{10}A - r_k \ + D - s_{j\,,} \tag{8}$$

and from (5)

$$\log_{10}A - r_k \ - s_j \ = b_i \ + c, \tag{9}$$

so that for the i-th earthquake

$$ML = b_i + c + D. \tag{10}$$

3 DISTANCE AND STATION EFFECTS ON *ML* VALUES

3.1 Analysis of variance study

Measurements of the maximum amplitude recorded on vertical and N-S and E-W oriented horizontal seismometers were made from 40 UK earthquakes in the period 1996-2002, as recorded at 28 three-component stations in the BGS UK seismograph network. Examination of the arrival time, signal character, and particle motion of these waves indicates that they are predominantly *Lg* waves, arriving shortly after the *Sg* phase and showing no dispersion. The locations of the earthquakes and stations are shown in Figure 1, together with the propagation paths corresponding to the seismograms. The propagation paths mainly sample the western and central parts of the UK, with reasonably good north to south coverage. At least three stations recorded each earthquake. Four stations (BCC, HBL2, KEY2, LDU) are strong motion accelerometer stations. The range of distances was 0-600km and this range was divided up into 30 intervals of 20km length. As stated in section 1, BGS has consistently estimated *ML* using the average of the magnitudes formed from the maximum wave amplitudes recorded on two orthogonal horizontal (H) seismometers, and the amplitudes and measurements of *ML* are published in their annual bulletins of seismicity for the UK. The present study has analysed individual horizontal component wave amplitudes, as well as mean horizontal wave amplitudes, at each station. It has also used vertical (Z) component amplitudes in order to determine if consistent local magnitudes can be determined from vertical records alone. Use of vertical records would allow more stations to contribute to magnitude determination, since there are many more vertical stations than three-component stations in the BGS network. This is useful when small events generate measurable seismograms at only a few stations, since only one or none of these may be three-component stations.

It was noted in Section 1 above that systematic differences arise between magnitudes calculated from average component magnitudes, and magnitudes calculated from the average component amplitude. Both magnitudes were calculated for station data used in the analysis of variance, and the values were compared. The average difference between the magnitudes over all the earthquakes was 0.007 units, the largest difference for a single earthquake was 0.019, and the largest difference for a single station measurement was 0.057 (the average amplitude magnitude being greater). Thus the systematic differences between the magnitude calculation procedures are not likely to be significant when magnitude is calculated using records from three or more stations.

The analysis of variance procedure described in section 2 above was applied to the data using a computer program developed by A Douglas (Carpenter et al. 1967). The program generates tables of station effects s_j and distance effects r_k for the stations, and distance intervals, respectively. Application of Snedecor's F-test (Abramowitz & Stegun, 1972) to the station and distance variances shows that both are highly significant at the 0.1 percent level, for both horizontal and vertical component data. The statistics associated with the analysis are presented in Table 1. The variation of amplitude with distance (r in equation 1) for horizontal and vertical amplitude measurements is shown in Figure 2, and the station corrections S are given in Table 2, calculated for the average component amplitudes.

Station corrections calculated for individual components were also calculated, but the differences between them and the average amplitude corrections were not significant. The NS and EW horizontal component corrections differed by more than 0.2 magnitude units from the average amplitude station correction at only the most northerly station (LRW), and at 23 stations out of 28 the difference was less than 0.1

3.2 Calibration of distance effect for Richter local magnitudes

It was noted in section 2 that a constant D must be added to the distance correction formed from r_k so that the magnitudes ML computed using the amplitude-distance curve derived from observed amplitudes agree on average with magnitudes computed by a specified agency. The baseline for the distance correction was chosen so that the magnitudes ML are defined according to the Richter definition of local magnitude, subsequently modified by Hutton & Boore (1987), so that a ML 3 earthquake corresponds to 10mm of displacement on a Wood Anderson (WA) seismometer at 17km hypocentral distance. This magnitude is denoted ML^R. In the UK, very few earthquakes are recorded at a distance of 17km, and so the equivalent original definition due to Richter (1935) is used, that a ML 3 earthquake will generate a 1mm displacement on a WA seismometer at 100km hypocentral distance. The WA gain is assumed to be 2080 (Bormann 2002), so that 1mm WA displacement corresponds to 481nm actual displacement, and a logA value of 2.68. Interpolating between the horizontal component distance effects determined for the ranges 80-100km, and 100-120km, yields the value of 0.81 for the distance effect r_k at 100km. It follows that for a ML value of 3 at 100km hypocentral distance, the constant D to be added to the distance correction, $-r_k$, to form the distance correction $B(\Delta)$, must be 1.13 for horizontal component measurements. A similar procedure yields a value of 1.08 for D for vertical component measurements. The distance correction $B(\Delta)^R$ for evaluating the Richter magnitude ML^R is given for both horizontal (H) and vertical (Z) components in Table 3.

BGS uses the Hutton & Boore (1987) distance correction when estimating ML for local earthquakes. We shall refer to this ML as ML^{HB}. The expression for ML^{HB}, specified for a measured displacement A in nm at distance Δ km, (e.g. Walker 2000), is

$$ML^{HB} = \log A + B(\Delta)^{HB} = \log A + 1.11 \log(\Delta) + 0.00189 * \Delta - 2.09 \qquad (11)$$

The $B(\Delta)^R$ distance corrections and the Hutton & Boore (1987) corrections $B(\Delta)^{HB}$ used to compute ML^{HB} are compared in Figure 3. Discrepancies in the range 40-80km and 400-440 km are believed to reflect real differences in *Lg* wave propagation in the UK compared to California. Over the range 90 to 400 km the corrections are very similar, implying that the crustal attenuation properties of Southern California and the UK are similar for S-waves and *Lg* waves. This is an unexpected discovery, as the geology and tectonics are quite different.

ML^R values were calculated for each station and each earthquake which contributed the amplitude values used in the analysis of variance study, using equation 8 above, for both horizontal and vertical component amplitude values. Corresponding estimates of ML^{HB} were determined from the same amplitude values. The mean earthquake magnitudes ML^R and ML^{HB}, and the corresponding standard deviations, are listed in Table 4 and $ML^R(H)$ is plotted against ML^{HB} for each earthquake in Figure 4. (ML^R - ML^{HB}) varies between 0.22 and –0.05 magnitude units, and 0.19 and –0.09 magnitude units, for horizontal and vertical component data, respectively. The respective average difference is 0.07 and 0.05 magnitude units. Note that the standard deviations of the sets of ML^R values for each earthquake are usually smaller than the standard deviations of the ML^{HB} values, and 35 standard deviations exceed 0.2 for ML^{HB} compared to only 4 for ML^R, which indicates that ML^R is more consistent than ML^{HB}. The similarity between the distance corrections used for ML^{HB} and ML^R suggests that this is almost entirely due to the use of station corrections in the calculation of ML^R. It is seen that $ML^R(H)$ is larger than $ML^R(Z)$ by about 0.2 magnitude units; this is due to the slight differences in the amplitude-distance curves for horizontal and vertical component amplitudes, after applying the definition of ML at 100km distance. $ML^R(H)$ is plotted against $ML^R(Z)$ in Figure 5; the best fitting straight line to this plot, assuming the gradient is unity, provides the following equation

$$ML^R(H) = ML^R(Z) + 0.21, \tag{12}$$

which allows a consistent magnitude to be determined from a combination of horizontal and vertical component records. Since the baseline for the ML^R scale has been set according to values for displacement for a specified magnitude observed in California, the ML^R magnitudes will still be biased with respect to those determined by independent global body and surface wave magnitude scales.

3.3 Calibration of distance effect for IDC magnitudes

The constant D can also be computed so that the computed ML will be equivalent to the teleseismic body wave magnitude m_b in the Reviewed Event Bulletin (REB) published by the International Data Centre (IDC) of the Comprehensive Test-Ban Treaty Organisation. Source parameters for seven earthquakes occurring in the UK region have been published in the IDC REB. The location accuracy of four of these earthquakes is relatively poor, as they occurred offshore, hence distance values for them may be inaccurate. Of the remaining three earthquakes, one (5 in Table 5) was assigned an m_b by only one IDC station, and the remaining two (1, 8 in Table 5) from observations at three or more IDC stations at different azimuths and distances. Of the latter two earthquakes, I used the larger magnitude earthquake *(*m_b 4.0) to calibrate the distance effect for IDC m_b *(*m_b^{IDC}*)*, to avoid the possibility that background noise might bias the IDC estimate at the low magnitude of m_b 3.3. The correction factors to be applied to calculate m_b^{IDCML} from horizontal amplitude values are given in Table 3.

In order to determine whether m_b^{IDCML} is consistent with the m_b^{IDC} values, the station and source corrections were used to estimate m_b^{IDCML} for seven local earthquakes for which m_b^{IDC} estimates are available. These estimates, together with ML^R calculated using the corrections derived above, are presented in Table 5. Estimates of m_b computed by the US NEIC and ISC are also provided where available. For one earthquake, there is an NEIC m_b but not an IDC m_b. Discrepancies may occur between NEIC and IDC magnitudes, which depend on source type, source depth, and magnitude, and are due to differences in the procedures used by the two agencies to calculate m_b (Murphy & Barker 2003). For the earthquakes used here, the IDC m_b magnitudes are consistently lower than the NEIC m_b estimates, by about 0.3-0.4 magnitude units on average. Data from four of the earthquakes (1, 5, 6 and 8) were used in the above determination of the station and distance corrections. Table 5 shows that the m_b^{IDCML} estimates are generally close to m_b^{IDC}. A significant discrepancy of 0.4 magnitude unit is observed between m_b^{IDCML} and m_b^{IDC} for earthquake 5. This earthquake occurred in the Bristol Channel and m_b^{IDC} was determined by a single station (ARCES). ML as determined by IDC from records at distances less than 20º was 3.3, and the earthquake did not appear in the NEIC bulletin. Thus it is likely that the true magnitude is lower than 3.6 and the m_b^{IDC} estimate is biased high due to path and site effects associated with this single station, or contamination by background noise at low signal amplitude.

The corrections in Table 3 give an m_b^{IDCML} equivalent to m_b^{IDC}. Other relations have been determined which give teleseismic m_b from local seismograms in the UK. Jacob & Neilson (1977) provided a scale to measure m_b^*, equivalent to teleseismic m_b, at ranges as short as 200km. The equation is

$$m_b^* = \log V + 2.3\log R - 2 \tag{13}$$

where V is the ground velocity represented by the maximum trace amplitude in the P-wave train in microns per second and R is the distance in km. Jacob & Neilson (1977) matched m_b^* to ML (equivalent to ML^R) with the relation

$$ML = 0.72\, m_b^* + 1 \tag{14}$$

using a dataset consisting of low magnitude British earthquakes observed in central Scotland. A subsequent study by Neilson and Burton (1985), using data from higher magnitude onshore British earthquakes, produced the relation

$$ML = 0.98\, m_b^{*} + 0.31 \qquad (15)$$

Values m_b^{*JN} and m_b^{*NB} derived from (13) and (15) above are shown in Table 5. Measured values of m_b^{*} from P-wave measurements on BGS UK stations show a large standard deviation, which is probably due to the asymmetry of the *P*-wave radiation pattern for earthquakes. Estimates of m_b^{*} obtained from values of ML^{R} are better matched to m_b^{IDC} and m_b^{NEIC}, and have a much smaller standard deviation, than estimates from *P*-wave velocity measurements. This is because *Lg*-wave radiation for earthquakes shows less azimuthal variation than *P*-wave radiation. The m_b^{*} values lie between m_b^{IDC} and the NEIC m_b values, generally nearest m_b^{IDC}, but this is probably not significant since Jacob & Neilson (1977) found that the difference between m_b (NEIC) and m_b^{*} could be of the order of 0.3 magnitude units, and Table 5 shows that for some earthquakes it can be even higher. For UK earthquakes it seems to be more reliable to scale to teleseismic m_b using *ML* rather than m_b^{*}.

The absence of data from underground explosions recorded by BGS and the IDC together has meant it has not been possible to compare m_b^{IDCML} with an IDC value of m_b for such explosions. However, in studies of Nevada and Semipalatinsk explosions, Nuttli (1986) and Ringdal et al. (1992) respectively have shown that *Lg*-based source size estimators are reliable and provide a stable estimate of magnitude, and that these estimates show significantly less scatter between station pairs than estimates of m_b (Hansen et al. 1990). Thus I believe that there is no reason to suggest that the relation derived above will not be applicable to underground explosions.

3.4 Discussion

It is difficult to interpret the variation in station effect between stations in terms of shear-wave (S_g and L_g) propagation characteristics. The station corrections in Table 2 differ significantly within groups of nearby stations and between horizontal and vertical components at individual stations. For example, the groups of nearby stations (BCC, BHH, ESK), (MCH, SSP, HBL2), (CWF, KEY2), and (HPK, LDU) all show wide disparity between horizontal station corrections, and BHH, CR2, HPK, MCH and ORE show very different sizes of correction for horizontal and vertical amplitudes.

Note that due to variations in the number of data samples at the different stations and distance ranges, the corrections are not equally well constrained. The strong motion stations provided recorded amplitudes only for the largest magnitude earthquakes, and in the 0-600km distance range only two measurements were available at the northernmost station at Lerwick (LRW). Distances were well sampled from 20 km to 400km; only the largest earthquakes generated measurements beyond 400km.

4 ESTIMATION OF QUALITY FACTOR, Q

After applying a correction for geometrical spreading, it is possible to use the decay of log A to derive an expression for the attenuation due to anelastic absorption and the quality factor Q. Nuttli (1973) proposed that the amplitude decay A(Δ) of the vertical component *Lg* wave with epicentral distance Δ can be written:

$$A(\Delta) = A_0\, \Delta^{-n}\ \exp(-k\Delta), \tag{16}$$

at small distances where earth curvature can be neglected, where A_0 is a factor independent of distance. Δ^{-n} describes attenuation due to geometrical spreading and $\exp(-k\Delta)$ describes attenuation due to anelastic absorption and scattering. Nuttli (1973) suggested that n=5/6, which is appropriate for a non-dispersive Airy phase trapped in the crustal waveguide in the time domain. If Δ is in km, the attenuation coefficient $k = \pi/QUT$, where Q is the specific quality factor for waves of period *T,* and *U* is the group velocity of the waves. Bowman & Kennett (1991) note that if the Moho is a gradient zone rather than a first order discontinuity, the amplitude decrease due to geometrical spreading may not obey a simple power law. Then it is difficult to separate the effect of geometrical spreading and those of anelastic absorption and scattering. In this work we make the assumption that the effects can be separated as in equation (16), and note from Bowman & Kennett (1991) that Q may then be underestimated, so that the derived value of Q would be a lower limit on the average Q for the UK for the average frequency at which Lg amplitudes are observed (f = 2.85Hz). For a given value of the period, the decay of log A with distance, with a correction for geometrical spreading is, from (16):

$$r(\Delta) + 0.833 \log \Delta = -0.4343\, k\Delta + \text{constant}. \tag{17}$$

Thus when the decay of log A is corrected for geometrical spreading, the resulting curve should show a linear decay with Δ. The corrected values of log A plotted against distance are shown in Figure 6, and it is seen that the curve is approximately linear with a slope of 0.29 ± 0.03 degree^{-1}, giving k as 0.668 degree^{-1}. For the average *Lg* wave period observed on the short period seismograms, T = 0.35sec, f=2.85hz, and assuming a group velocity U = 3.4 km sec^{-1}, the specific quality factor Q is 440 ± 50.

From independent spectral measurements, Sargeant & Ottemöller (2006, personal communication) have derived the expression $Q = 337(f/1.58)^{0.45}$ for frequency-dependent Q in the UK; for T=0.35s, f=2.85hz, Q is 440, which matches the estimate derived from the amplitude-distance curve. It was noted that the corrections for distance in the 90-400km range are very similar to the Hutton & Boore (1987) corrections, which suggests that average *Lg* Q for the UK is similar to that for Southern California. This is corroborated by spectral measurements of *Lg* for southern California derived by Benz et al. (1997), who deduced the frequency-dependent function $Q = A(f/1.5)^{0.59(\pm 0.11)}$ for frequencies f = 1.0 to 7.0 hz, where A ranges between a minimum of 256 and a maximum of 313. The average UK value found above (Q = 440 ± 50) falls within the range Q = 345 to Q = 491 according to Benz et al. (1997), for f = 2.8 hz.

The similarity between *Lg* Q for the UK and Southern California was not expected, since the latter is an active tectonic region whereas the UK is not. Similar unexpectedly low values of *Lg* Q were found by Bowman & Kennett (1991) in central Australia and Frankel et al. (1990) in South Africa. More relevantly in a geographical context, low values of *Lg* Q have been found in France (Campillo & Plantet, 1991). Bowman & Kennett (1991) showed that when the Moho is a gradient zone and not a first order discontinuity, as under central Australia, the actual geometrical spreading may differ significantly from the simple power law $\Delta^{-5/6}$. The Q determinations are sensitive to small changes in the geometrical spreading exponent (Frankel et al. 1990).

In the UK, the Moho is a relatively sharp interface (Clegg & England, 2003), but there are strong lateral variations in crustal velocity structure (Barton 1992, Clegg & England 2003). These may cause significant frequency-dependent wave scattering, which would increase attenuation above that of geometrical spreading and anelastic attenuation. Campillo & Plantet

(1991) showed a strong correlation between the attenuation of the multiply reflected *Lg* crustal phases and heterogeneity in the lower crust of NW France, as observed by a wide-angle reflection profile. Thus I suggest that wave scattering is likely to play an important part in explaining the attenuation of *Lg* waves in the UK.

5 CONCLUSIONS

An analysis of shear-wave amplitudes from local earthquakes at stations of the UK seismic monitoring network has generated correction tables which allow the estimation of local magnitudes which are fully consistent with the Richter definition of local magnitude, as well as magnitudes which are equivalent to the body wave magnitudes published in the bulletins of the CTBTO International Data Centre. 385 amplitude readings from 40 local earthquakes recorded at 28 three-component seismometer stations and strong-motion accelerometer stations in the distance range 0-600km were used in this study. The effects on amplitude of source size, distance and near-station characteristics were separated using an analysis of variance technique. The new amplitude-distance curve and station corrections allow an estimate of m_b (IDC) from local shear-wave data which can be applied to event discrimination studies. It should be noted that the NEIC and IDC do not calculate body wave magnitude m_b in the same way. Thus when comparing body wave magnitudes of UK earthquakes, m_b^{IDC} and m_b^{IDCML} may be underestimated by 0.3-0.4 units when compared with NEIC magnitudes.

Local magnitude estimates of ML^R determined according to the Richter definition of local magnitude, using appropriately adjusted distance correction tables from the new amplitude-distance curve and the new station corrections, show a smaller variance than the corresponding BGS values calculated from the Hutton & Boore (1987) formula. This is due to the application of station corrections to the calculation of *ML*, which have not been included up until now in the standard BGS procedure for determining local magnitude. Since the distance corrections closely match those of Hutton & Boore (Figure 3), adoption of the new corrections will produce average magnitude estimates with smaller variance but no perceptible change in magnitude level.

After correcting for geometrical spreading following Nuttli (1973), the variation of wave amplitude with distance curve produces an estimate of average *Lg* Q of 450 , which is similar to that of Southern California and other active tectonic zones. The UK is not an active tectonic zone, and so this relatively low value was not expected. Since there appears to be no reason to assume that the geometrical spreading factor of r-5/6 for *Lg* waves is smaller in the UK, or that low-Q material exists in the crust, it is suggested that scattering from crustal heterogeneities under the UK is a significant factor in *Lg* wave attenuation in the crust.

ACKNOWLEDGEMENTS

The author thanks Professor Alan Douglas for stimulating discussions and advice on the topic of this report, and Alan and his colleague Mr John Young (AWE) for supplying the analysis of variance program used in this study. Peter Marshall, Neil Selby (AWE), Brian Baptie, Lars Ottemöller (BGS), and anonymous reviewers are also thanked for comments which significantly improved it. This paper is published with the permission of the Executive Director of the British Geological Survey (NERC).

REFERENCES

Abramowitz, M. & Stegun, I.A., 1972. *Handbook of mathematical functions*. Dover Publications, Inc. New York.

Barton, PJ, 1992, LISPB revisited; a new look under the Caledonides of northern Britain: *Geophys.J.Int.*, **110,** 371–391.

Benz, H.M., Frankel, A., & Boore, D.M., 1997. Regional Lg attenuation for the continental United States, *Bull.Seism.Soc.Am.*, **87,** 606-619.

Booth, D.C., Marshall, P.D. & Young J.B., 1974. Long and short period *P*-wave amplitudes from earthquakes in the range 0-114˚, *Geophys.J.R.astr.Soc.,* **39,** 523-537.

Bormann, P., 2002. Magnitude of seismic events. *IASPEI New Manual of Seismological Observatory Practice*. Bormann, P. (editor). Potsdam: GeoForschungsZentrum. ISBN 3-9808780-0-7.

Bowman, J.R. & Kennett, B., 1991. Propagation of *Lg* waves in the North Australian craton: influence of crustal velocity gradients, *Bull.Seism.Soc.Am.*, **81,** 592-610.

Brune, J. (1962) Attenuation of dispersed wave trains, *Bull.Seism.Soc.Am.*, **52,** 109-112.

Burton, P.W. (1974). Estimations of Q_γ^{-1} from seismic Rayleigh waves, *Geophys.J.R.astr.Soc.,* **36,** 167-189.

Campillo, M. & Plantet, J.L., 1991. Frequency dependence and spatial distribution of seismic attenuation in France: experimental results and possible interpretations, *Phys. Earth Planet. Int.*, **67**, 48-64.

Carpenter, E.W., Marshall, P.D. & Douglas, A., 1967. The amplitude-distance curve for short period teleseismic *P*-waves, *Geophys.J.R.astr.Soc.,* **13,** 61-70.

Clegg, B., & England, R.W. 2003. Velocity structure of the UK from a compilation of wide-angle and refraction data. *Geol. Mag.*, **140**, 453-467.

Ewing, M., Jardetzky, W.S., & Press, F., 1957. *Elastic waves in layered media*, McGraw-Hill, New York.

Frankel, A., McGarr, A., Bicknell, J., Mori, J., Seeber, L., & Cranswick, E., 1990. Attenuation of high-frequency shear waves in the crust: measurements from New York State, South Africa and Southern California, *J.Geophys. Res.*, **95**, 17441-17457.

Hansen, R.A., Ringdal, F., & Richards P.G., 1990.The stability of RMS Lg measurements and their potential for accurate estimation of the yields of Soviet underground nuclear explosions, *Bull.Seism.Soc.Am.*, **80,** 2106-2126.

Herrmann, R.B., 1980. Q estimates using the coda of local earthquakes, *Bull.Seism.Soc.Am.*, **70,** 447-468.

Hutton, K.L. & Boore, D.M., 1987. The ML scale in southern California: *Bull.Seism.Soc.Am.*, **77,** 2074-2094.

Jacob, A.W.B., & Neilson, G., 1977. Magnitude determination on LOWNET, *British Geological Survey Global Seismology Unit Report No. 206*, 40pp.

Marshall, P.D. & Basham, P.W., 1972. Discrimination between earthquakes and explosions employing an improved M_S scale, *Geophys.J.R.astr.Soc.,* **28,** 431-458.

MacBeth, C.D. & Burton, P.W., 1985. Upper crustal shear velocity models from higher mode Rayleigh wave dispersion in Scotland, *Geophys.J.R. astr. Soc.*, **83,** 519-539.

MacBeth, C.D. & Burton, P.W., 1986. Propagation of 0.7-2.5 Hz Rayleigh waves in Scotland, *Geophys.J.R.astr.Soc*., **84,** 101-120.

MacBeth, C.D. & Burton, P.W., 1987. Single-station attenuation measurements of high frequency Rayleigh waves in Scotland, *Geophys J.R.astr.Soc*., **88,** 757-798.

MacBeth, C.D. & Burton, P.W., 1988. Surface waves generated by underwater explosions offshore Scotland, *Geophys.J.R.astr.Soc.,* **94,** 285-294.

Murphy, J.R. & Barker, B.W., 2003. Revised Distance and depth Corrections for use in the estimation of short-period p-wave magnitudes, *Bull.Seism.Soc.Am.,* **93,** 1746-1764.

Neilson, G. & Burton, P.W., 1985. Instrumental magnitudes of British Earthquakes, in 'Earthquake Engineering for Britain', pp 83-85, Thomas Telford Ltd., London.

Nuttli, O.W., 1973. Seismic wave attenuation and magnitude relations for eastern North America, *J.Geophys.Res.,* **78,** 876-885.

Nuttli, O.W., 1886. Yield estimates of Nevada test site explosions obtained from seismic Lg waves, *J.Geophys.Res.,* **91,** 2137-2151.

Ottemoller, L., Shapiro, N.M., Singh, S.K., & Pacheco, J.F., 2002. Lateral variation of Lg wave propagation in southern Mexico, *J.Geophys.Res.,* **107,** 2008, doi:10.1029/2001JB000206.

Richter, C.F., 1935. An instrumental earthquake magnitude scale. *Bull.Seism.Soc.Am.*, **25,** 1-32.

Ringdal, F., Marshall, P.D., & Alewine, R.W., 1992. Seismic yield determination of Soviet underground nuclear explosions at the Shagan River test site, *Geophys.J.Int.*, **109,** 65-77.

Walker, A.B. (ed.), 2000. *Bulletin of British earthquakes 2000*, British Geological Survey Technical Report WL/00/01.

FIGURE CAPTIONS

Figure 1. Map showing propagation paths between earthquakes (black dots) and three-component UK seismometer stations (triangles), corresponding to the seismograms used in the analysis of variance study.

Figure 2. Amplitude-distance variation of shear-waves in the UK region, from mean maximum amplitudes in horizontal (H) and vertical (Z) component records. The 95% confidence limits at each 20km distance interval are indicated for the H values by horizontal bars.

Figure 3. Comparison of distance corrections $B(\Delta)^{HB}$, and $B(\Delta)^{R}$ for horizontal (H) and vertical (Z) amplitude measurements with associated error bars for H corrections, for the distance range 0 – 600km.

Figure 4. Comparison of $ML^{R}(H)$ and ML^{HB} for the earthquakes used for the analysis of variance study (values given in Table 5). The straight line fit to the data has a slope of 1.02 and an intercept of -0.14.

Figure 5. Comparison of $ML^{R}(H)$ and $ML^{R}(Z)$ for the earthquakes used for the analysis of variance study (values given in Table 5). The straight line fit to the data has a slope of 0.98 and an intercept of 0.25.

Figure 6. Decay of log (Amplitude) with distance after correction for the effects of geometrical spreading and dispersion, following Nuttli (1973). The straight line fit to the data has a slope of -0.29 and an intercept of 1.00.

Table 1 Statistics associated with analysis of variance of the horizontal and vertical amplitudes

	Horizontal	Vertical
Variance of a Single Observation	0.0265	0.0282
Total Degrees of Freedom	300	282
Sum of squares attributable to distance effect	47.325	41.484
Total degrees of freedom	29	28
Average square attributable to distance effect	1.632	1.482
Significance	<0.1%	<0.1%
Sum of squares attributable to station effect	9.553	3.322
Total degrees of freedom	27	25
Average square attributable to station effect	0.354	0.132
Significance	<0.1%	<0.1%
Constant	1.744	1.594

Table 2 Station Corrections with 95% confidence limits for application to log(Amplitude) measurements from horizontal (H) and Vertical (Z) component records. Strong motion stations are identified by an asterisk. Note that errors depend on the number of station records available.

Station	Correction (H)	Error (H)	Records used (H)	Correction (Z)	Error (Z)	Records used (Z)
BBO	0.03	0.07	29	0.06	0.07	29
BHH	-0.24	0.07	30	-0.05	0.07	29
BCC*	-0.02	0.20	3	0.09	0.18	4
BTA	-0.16	0.07	24	-0.01	0.07	24
CR2	0.22	0.12	9	0.01	0.12	9
CWF	0.16	0.09	17	0.16	0.09	17
DYA	-0.09	0.14	6	-0.11	0.15	6
EDI	0.12	0.08	21	0.19	0.08	18
ESK	0.23	0.07	23	0.04	0.08	22
GAL	0.22	0.08	18	0.07	0.09	17
GIM	0.19	0.07	25	0.05	0.07	25
HPK	-0.37	0.10	12	-0.08	0.11	11
HBL2*	-0.24	0.17	4	-0.20	0.20	3
HTL	0.05	0.10	12	-0.08	0.12	10
KEY2*	-0.36	0.20	4	-0.17	0.25	3
KPL	0.18	0.09	15	0.09	0.09	15
LDU*	-0.18	0.20	3			
LMI	0.12	0.07	25	0.00	0.07	24
LRW	0.07	0.40	2			
MCD	-0.07	0.10	14	-0.20	0.11	13
MCH	-0.03	0.09	14	0.18	0.10	13
ORE	-0.05	0.14	7	-0.23	0.14	7
PGB	0.04	0.09	17	0.13	0.09	16
RRR	0.15	0.13	7	0.10	0.14	7
SSP	0.16	0.09	16	0.05	0.09	16
SWN	-0.20	0.11	10	-0.20	0.12	9
TFO	-0.13	0.15	6	-0.04	0.15	6
WCB	0.21	0.08	23	0.15	0.08	22

Table 3 Distance corrections $B(\Delta)$ for application to log(Amplitude) measurements from horizontal (H) and vertical (Z) component records to calculate ML^R from horizontal (H) and vertical (Z) amplitudes, with 95% confidence limits, and m_b^{IDCML} from horizontal amplitudes.

Distance (km)	$B(\Delta)^R$ (H)	Error (H)	Records used (H)	$B(\Delta)^R$ (Z)	Error (Z)	Records used (Z)	$B(\Delta)^{IDC}$ (H)
0-20	-0.67	0.38	1	-0.76	0.43	1	-1.20
20-40	-0.26	0.13	9	-0.30	0.13	9	-0.79
40-60	0.19	0.10	16	0.20	0.10	15	-0.34
60-80	0.27	0.10	16	0.34	0.10	15	-0.26
80-100	0.25	0.09	19	0.28	0.10	17	-0.28
100-120	0.40	0.08	26	0.35	0.09	24	-0.13
120-140	0.42	0.08	31	0.43	0.08	30	-0.11
140-160	0.57	0.07	32	0.62	0.08	30	0.04
160-180	0.68	0.07	33	0.72	0.08	32	0.15
180-200	0.73	0.10	15	0.79	0.10	14	0.20
200-220	0.94	0.07	41	0.88	0.07	41	0.41
220-240	1.01	0.08	26	0.99	0.08	26	0.48
240-260	1.06	0.09	21	1.02	0.09	21	0.53
260-280	1.17	0.09	18	1.15	0.09	18	0.64
280-300	1.21	0.10	14	1.16	0.11	12	0.68
300-320	1.29	0.09	16	1.24	0.10	14	0.76
320-340	1.34	0.10	12	1.33	0.11	11	0.81
340-360	1.52	0.11	11	1.47	0.12	10	0.99
360-380	1.49	0.14	7	1.49	0.14	7	0.96
380-400	1.55	0.16	5	1.49	0.18	4	1.02
400-420	1.75	0.17	4	1.57	0.21	3	1.22
420-440	1.77	0.16	5	1.69	0.17	5	1.24
440-460	1.72	0.20	3	1.55	0.20	3	1.19
460-480	1.73	0.34	1	1.81	0.35	1	1.20
480-500	1.83	0.17	4	1.77	0.18	4	1.30
500-520	1.81	0.51	1	1.87	0.25	2	1.28
520-540	1.94	0.24	3				1.41
540-560	2.05	0.35	1	1.97	0.37	1	1.52
560-580	1.97	0.20	3	2.07	0.21	3	1.44
580-600	2.19	0.24	2	2.12	0.25	2	1.66

Table 4. Comparison of Richter local magnitudes ML^R and ML^{HB} and their standard deviations (S.D.) for all earthquakes used in the determination of station and distance corrections, for horizontal (H) and vertical (Z) component amplitude data.

Evt.DateTime	***ML^R* (H)**	**S.D.**	***ML^R* (Z)**	**S.D.**	***ML^HB* (H)**	**S.D.**	***ML^HB* (Z)**	**S.D.**
9603072341	3.54	0.1	3.35	0.15	3.4	0.23	3.32	0.16
9604211828	2.22	0.13	1.81	0.15	2.07	0.13	1.76	0.17
9605060349	2.93	0.14	2.69	0.14	2.8	0.23	2.58	0.18
9605182101	3.2	0.13	3.03	0.15	3.13	0.14	3	0.2
9609200404	2.88	0.15	2.71	0.19	2.87	0.27	2.72	0.2
9610150542	1.88	0.24	1.78	0.23	1.75	0.28	1.6	0.12
9702042212	2.62	0.12	2.46	0.16	2.56	0.17	2.43	0.16
9702102309	2.77	0.11	2.5	0.06	2.81	0.18	2.48	0.08
9705172149	2.28	0.1	2.04	0.08	2.11	0.11	1.91	0.2
9707300834	2.84	0.15	2.65	0.2	2.75	0.23	2.58	0.31
9708261957	2.76	0.17	2.57	0.16	2.66	0.28	2.48	0.21
9710190242	2.5	0.07	2.26	0.18	2.51	0.16	2.28	0.15
9711080446	2.47	0.14	2.21	0.11	2.42	0.22	2.23	0.19
9802080551	2.34	0.09	2.18	0.09	2.28	0.18	2.16	0.11
9802171426	2.32	0.12	2.15	0.15	2.3	0.26	2.03	0.23
9803262051	2.69	0.14	2.45	0.15	2.56	0.29	2.34	0.34
9805030212	3.61	0.13	3.44	0.15	3.55	0.17	3.39	0.16
9805311255	2.53	0.07	2.29	0.07	2.44	0.1	2.25	0.16
9807200738	2.69	0.07	2.44	0.06	2.63	0.17	2.4	0.08
9807210716	2.17	0.14	1.91	0.14	2	0.21	1.76	0.2
9807311055	2.09	0.15	1.9	0.11	2.12	0.2	1.85	0.13
9808082207	2.05	0.17	1.91	0.17	2	0.24	1.81	0.2
9809150232	2.42	0.18	2.23	0.11	2.2	0.17	2.08	0.11
9901211110	2.99	0.11	2.78	0.12	2.97	0.24	2.78	0.13
9903040016	3.71	0.08	3.5	0.13	3.69	0.24	3.49	0.16
9906170220	2.7	0.06	2.47	0.07	2.66	0.18	2.45	0.12
9909010500	3.22	0.14	3.07	0.09	3.14	0.17	3.04	0.11
9910020350	2.59	0.17	2.42	0.09	2.54	0.27	2.35	0.18
9910251915	3.73	0.16	3.5	0.12	3.61	0.23	3.44	0.13
0002120851	3.03	0.19	2.91	0.19	2.95	0.29	2.83	0.29
0004240510	2.64	0.16	2.45	0.12	2.52	0.23	2.35	0.19
0006221436	2.65	0.08	2.54	0.12	2.59	0.14	2.51	0.09
0008080246	2.45	0.21	2.32	0.21	2.43	0.3	2.31	0.23
0009230423	3.84	0.11	3.55	0.08	3.84	0.22	3.56	0.13
0102251239	2.2	0.13	1.99	0.11	2.18	0.12	1.93	0.11
0105130826	3.27	0.19	3.09	0.21	3.15	0.27	2.98	0.38
0105312342	3.74	0.12	3.47	0.15	3.66	0.18	3.43	0.12
0110281625	4.02	0.1	3.81	0.14	3.98	0.23	3.82	0.22
0209222353	4.54	0.19	4.45	0.14	4.6	0.3	4.54	0.12
0210211141	3.85	0.13	3.74	0.16	3.81	0.22	3.74	0.19

Table 5. Comparison of local magnitude ML^R and m_b^{IDCML} (equivalent to IDC m_b) with m_b magnitudes estimated by IDC, NEIC, ISC and m_b^* derived by measurement (Jacob & Neilson, 1977) and from ML^R (Neilson and Burton, 1985).

No.	Date	Time	Lat.	Long.	ML^R	m_b^{IDCML}	m_b^{IDC}	m_b^{NEIC}	m_b^{ISC}	m_b^{*JN}	m_b^{*NB}
1	23/09/00	04:23	52.280	-1.610	3.8	3.3	3.3		3.3	3.4	3.6
2	08/12/00	05:54	59.944	1.934	4.9	4.4	4.3	4.7	4.7	4.0	4.4
3	14/03/01	22:20	58.252	0.695	3.4	2.9	3.2	3.3	3.2	3.5	3.1
4	07/05/01	09:43	56.596	3.248	4.0	3.4	3.6	3.8	3.9	3.3	3.8
5	31/05/01	23:42	50.977	-4.531	3.7	3.2	3.6		3.6	3.3	3.5
6	28/10/01	16:25	52.846	-0.856	4.0	3.5	3.7	4.2		3.8	3.8
7	14/02/02	19:00	59.793	2.536	4.1	3.6		3.9	4.0	4.0	3.8
8	22/09/02	23:53	52.520	-2.150	4.5	4.0	4.0	4.8	4.5	3.8	4.4

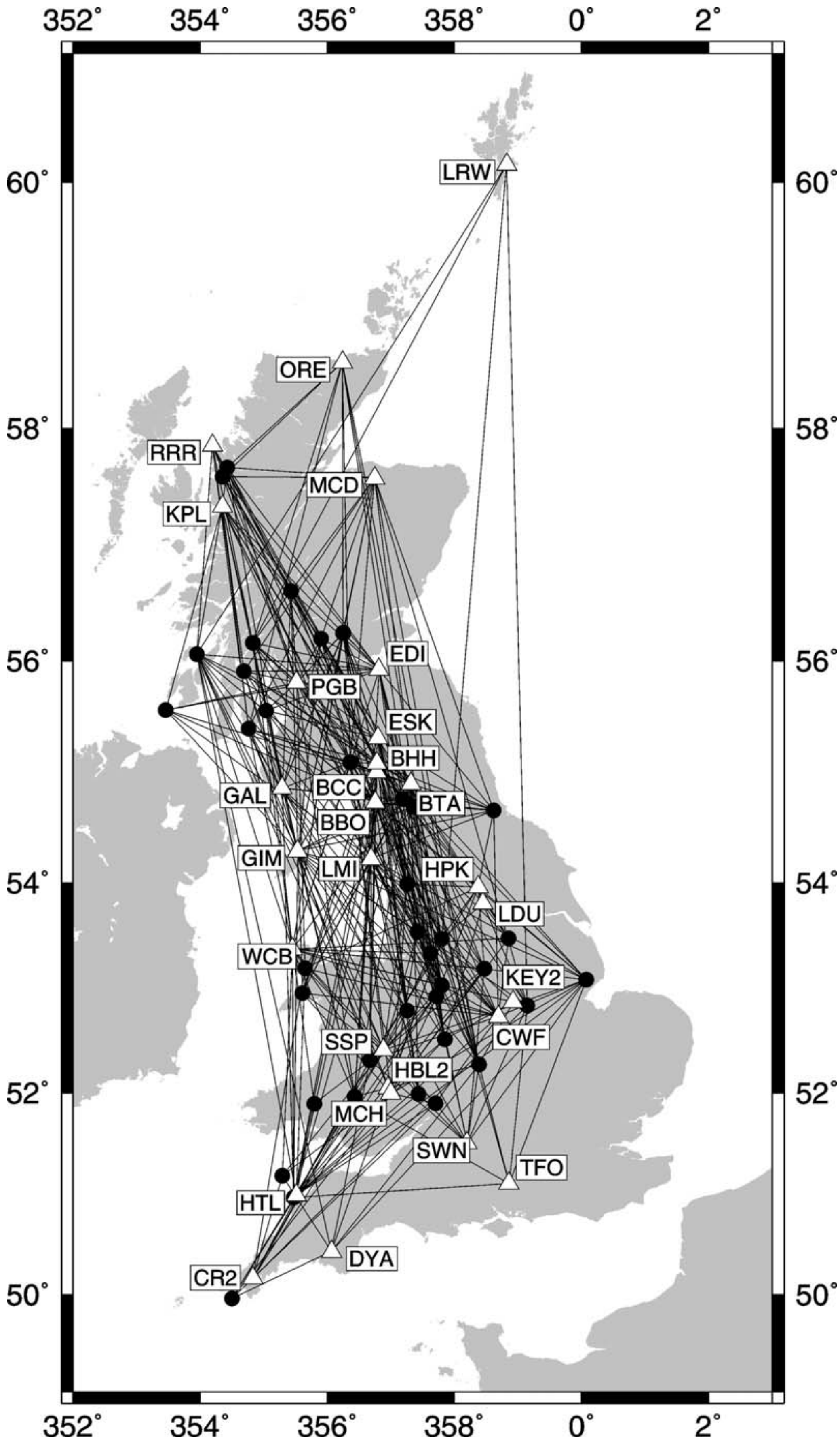

Figure 1. Map showing propagation paths between earthquakes (black dots) and three-component UK seismometer stations (triangles), corresponding to the seismograms used in the analysis of variance study.

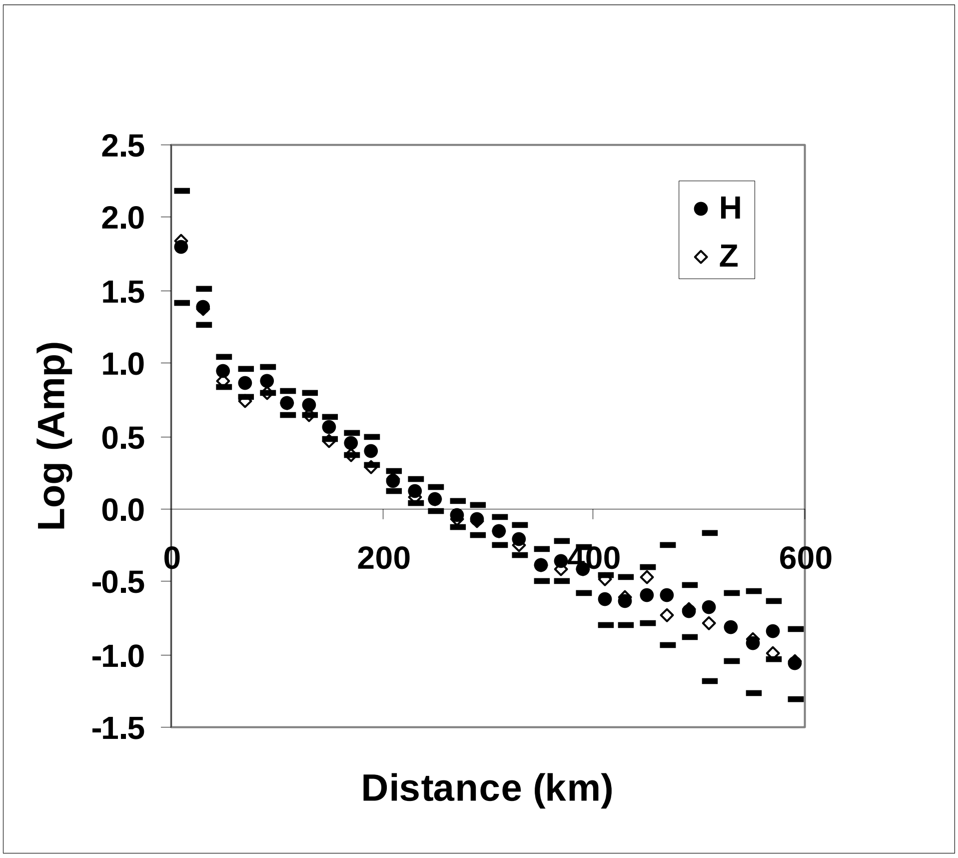

Figure 2. Amplitude-distance variation of shear-waves in the UK region, from mean maximum amplitudes in horizontal (H) and vertical (Z) component records. The 95% confidence limits at each 20km distance interval are indicated for the H values by horizontal bars.

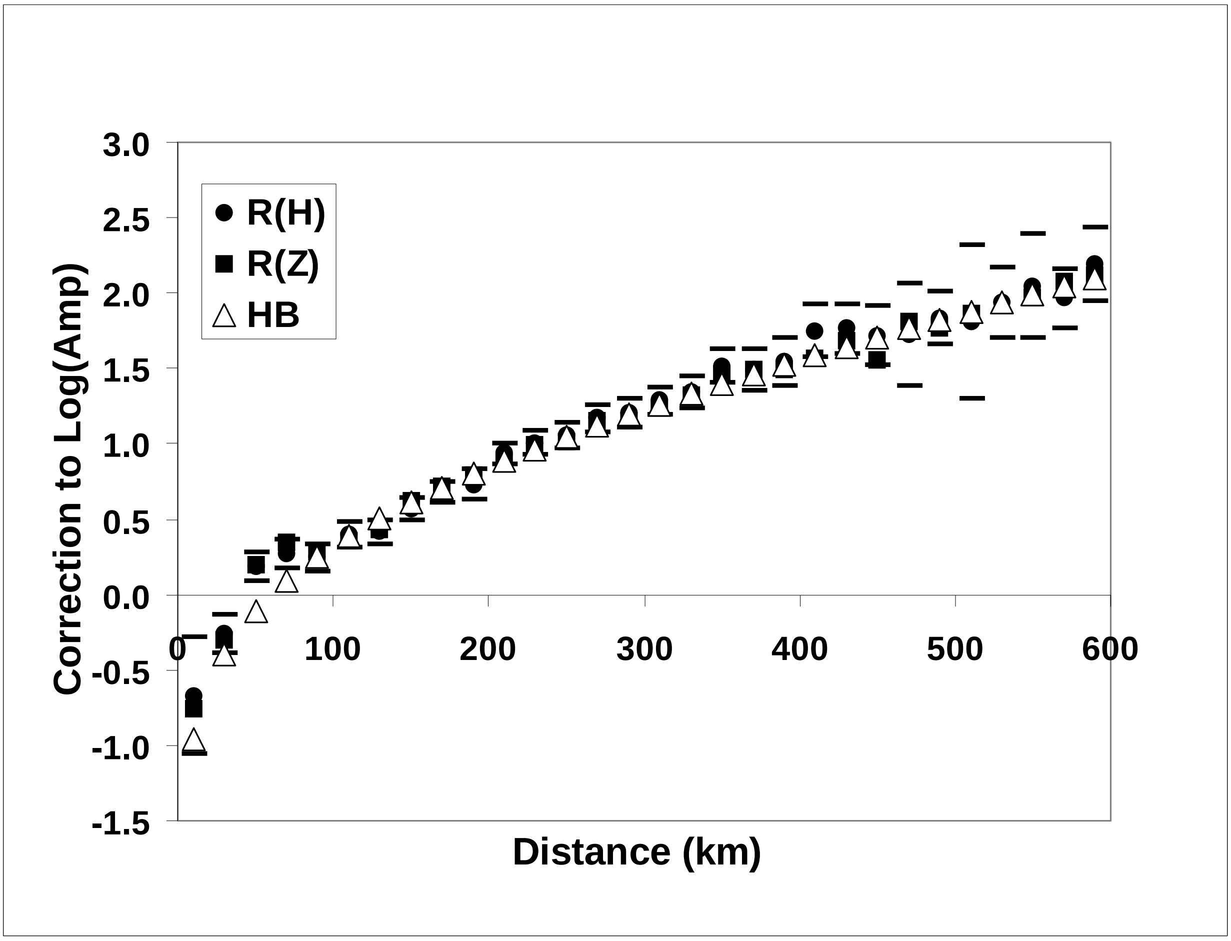

Figure 3. Comparison of distance corrections $B(\Delta)^{HB}$, and $B(\Delta)^{R}$ for horizontal (H) and vertical (Z) amplitude measurements with associated 95% confidence error bars for H corrections, for the distance range 0 – 600km.

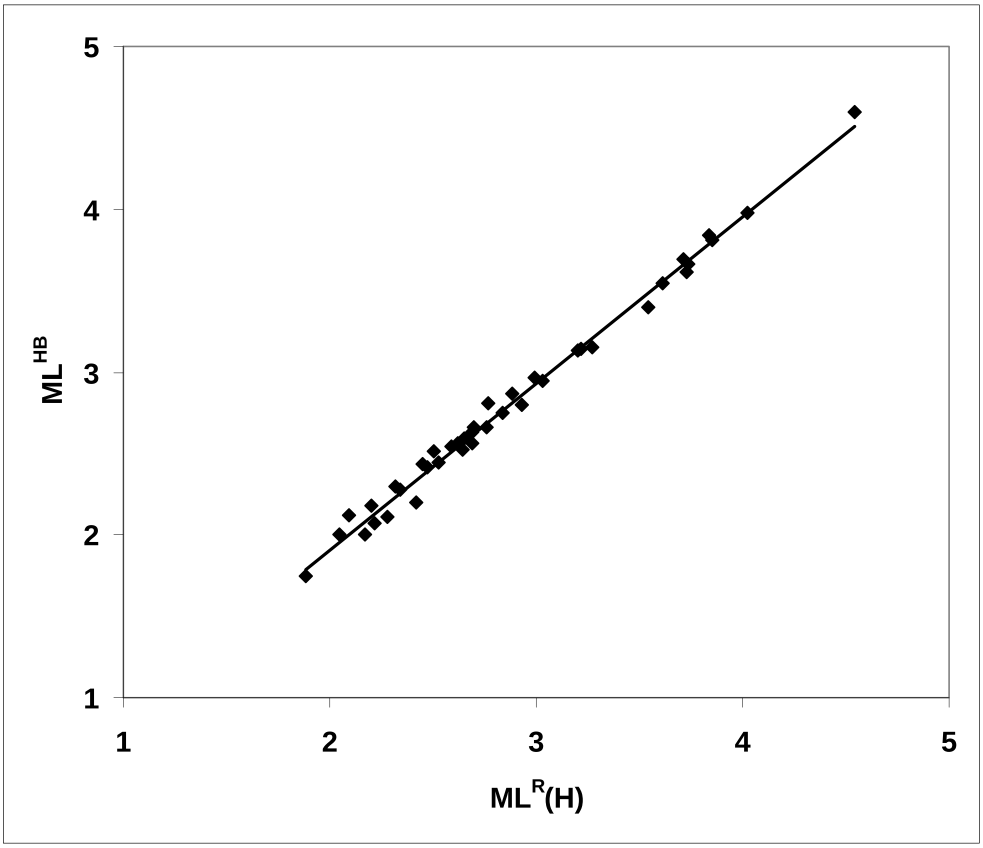

Figure 4. Comparison of $ML^{R}(H)$ and ML^{HB} for the earthquakes used for the analysis of variance study (values given in Table 5). The straight line fit to the data has a slope of 1.02 and an intercept of -0.14.

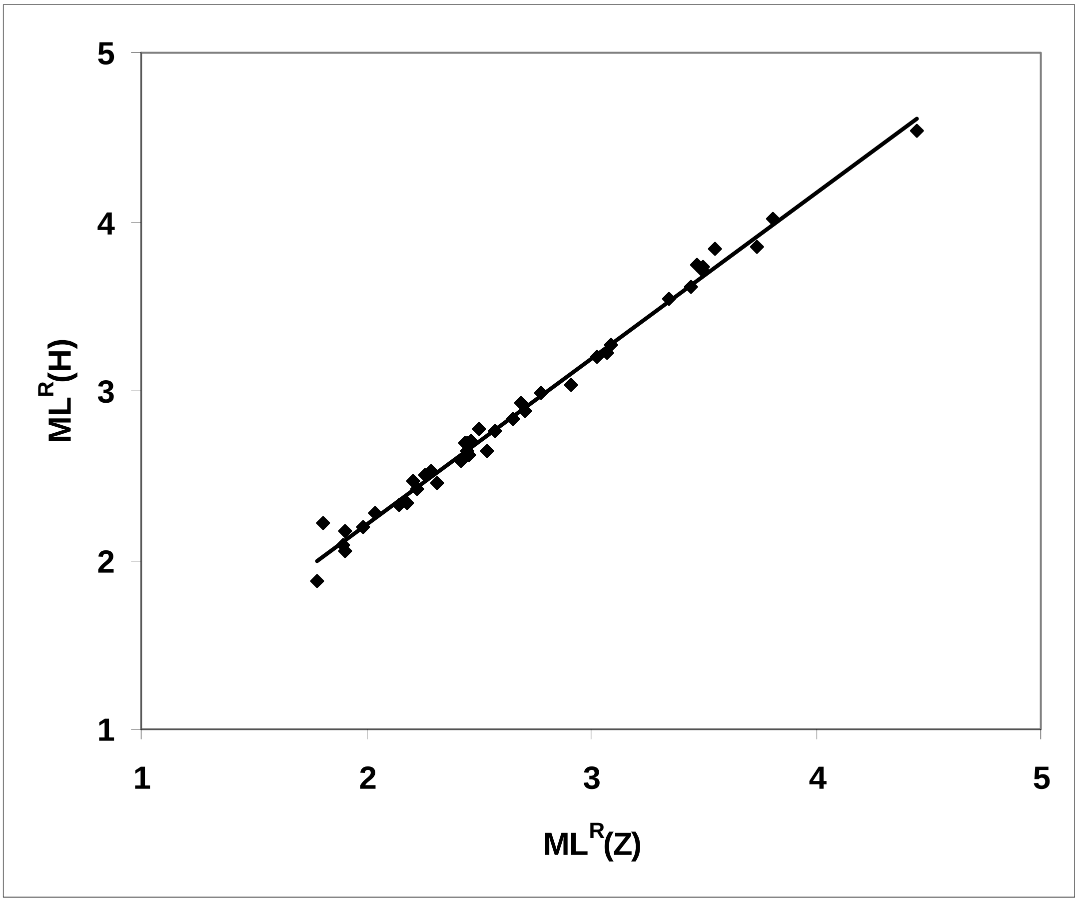

Figure 5. Comparison of $ML^R(H)$ and $ML^R(Z)$ for the earthquakes used for the analysis of variance study (values given in Table 5). The straight line fit to the data has a slope of 0.98 and an intercept of 0.25.

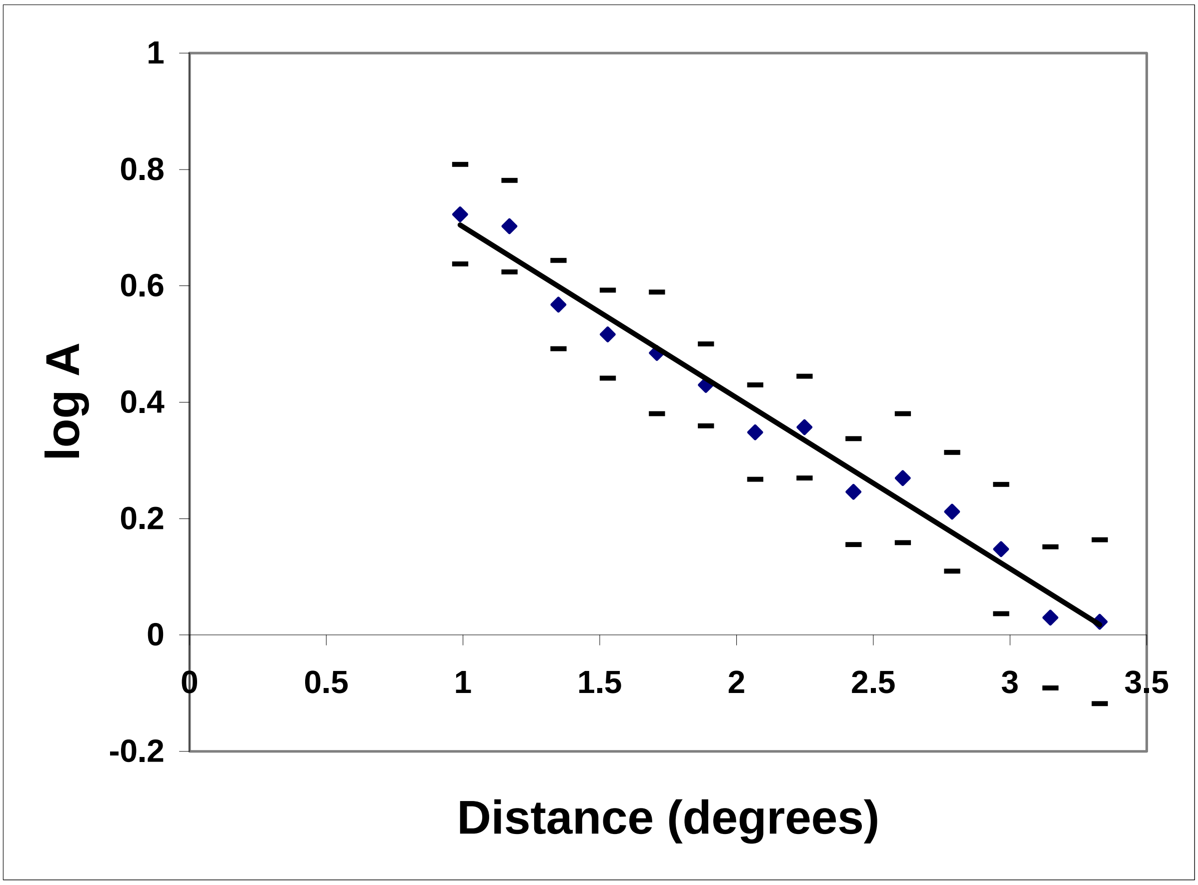

Figure 6. Decay of log (Amplitude) with distance after correction for the effects of geometrical spreading, following Nuttli (1973). The straight line fit to the data has a slope of -0.29 and an intercept of 1.00.